Supporting Information

DNA Functionalized Metal-Organic Framework Combing with Magnesium Peroxide Nanoparticles: Targeted and Enhanced Photodynamic Therapy

Xinran Sun, Guoda Zhang, Xilai Ding, Yingyan Liu, Kaixiu Chen, Pengfei Shi* and Shusheng Zhang*

Shandong Provincial Key Laboratory of Detection Technology for Tumor Markers, School of Chemistry and Chemical Engineering, Linyi University, Linyi 276000, Shandong, P. R. China.

Contents

Fig. S1. XPS high-resolution spectrum of Hf 4f in Hf-MOF-MgO_2/DNA. 2
Fig. S2. XPS high-resolution spectrum of Mg 1s in Hf-MOF-MgO_2/DNA. 2
Fig. S3. XPS spectra of Mg 1s in MgO_2, Hf-MOF and Hf-MOF-MgO_2/DNA. 3
Fig. S4. TEM image of MgO_2. 3
Fig. S5. PXRD patterns of MgO_2, Hf-MOF, Hf-MOF-MgO_2/DNA. 4
Fig. S6. Fluorescence spectra of DCFH incubated with MgO_2, Hf-MOF and Hf-MOF-MgO_2. 4
Fig. S7. UV-Vis absorbance of Hf-MOF by combining different amounts of MgO_2. 5
Fig. S8. UV-Vis absorbance of DNA before and after modification with Hf-MOF-MgO_2. 5
Fig. S9. Images of O_2 bubbles generated by the freshly synthesized MgO_2 and Hf-MOF-MgO_2/DNA. 6
Fig. S10. UV-Vis absorbance spectra of H_2TCPP ligands at different concentration. 6
Fig. S11 The calibration curve of absorbance at 418 nm and the concentration of H_2TCPP. 7
Fig. S12. Confocal images of calcein AM and PI co-stained 4T1 cells under normoxia conditions. 7
Fig. S13. Confocal images of calcein AM and PI co-stained 4T1 cells under hypoxia conditions. 8
Fig. S14. Confocal images of calcein AM and PI co-stained A549 cells under normoxia conditions. 8
Fig. S15. Confocal images of calcein AM and PI co-stained A549 cells under hypoxia conditions. 9
Fig. S16. Confocal images of Calcein-AM/PI stained 4T1 and A549 cells without light irradiation. 9
Fig. S17. Confocal images of ROS generation in 4T1 and A549 cells without light irradiation. 10
Fig. S18. The fluorescence imaging of mice and major organs. 10
Fig. S19. Tumor weight of different groups after treatment. 10

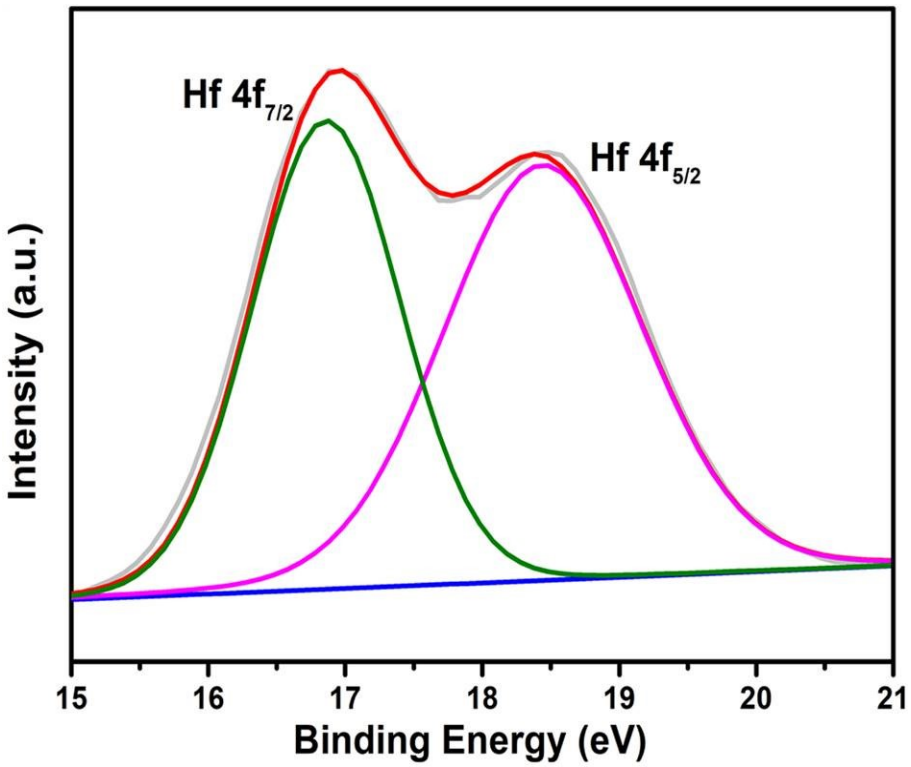

Fig. S1. XPS high-resolution spectrum of Hf 4f in Hf-MOF-MgO_2/DNA.

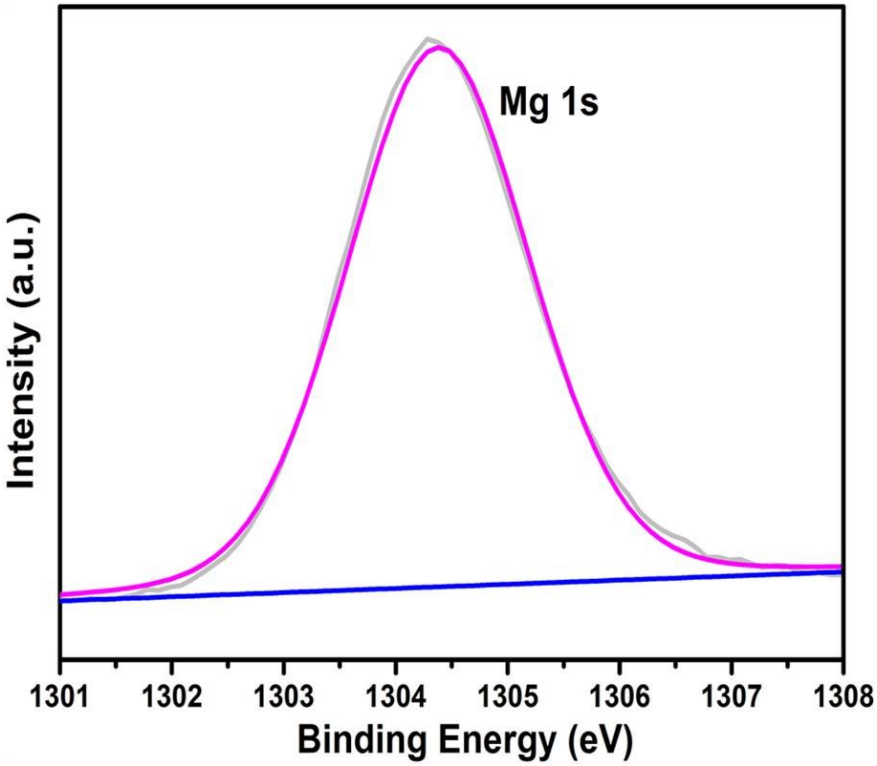

Fig. S2. XPS high-resolution spectrum of Mg 1s in Hf-MOF-MgO_2/DNA.

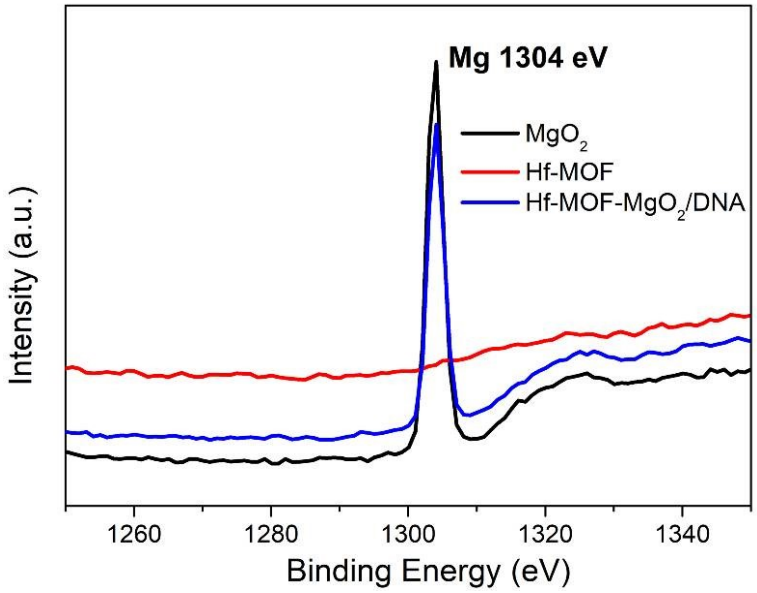

Fig. S3. XPS spectra of Mg 1s in MgO_2, Hf-MOF and Hf-MOF-MgO_2/DNA.

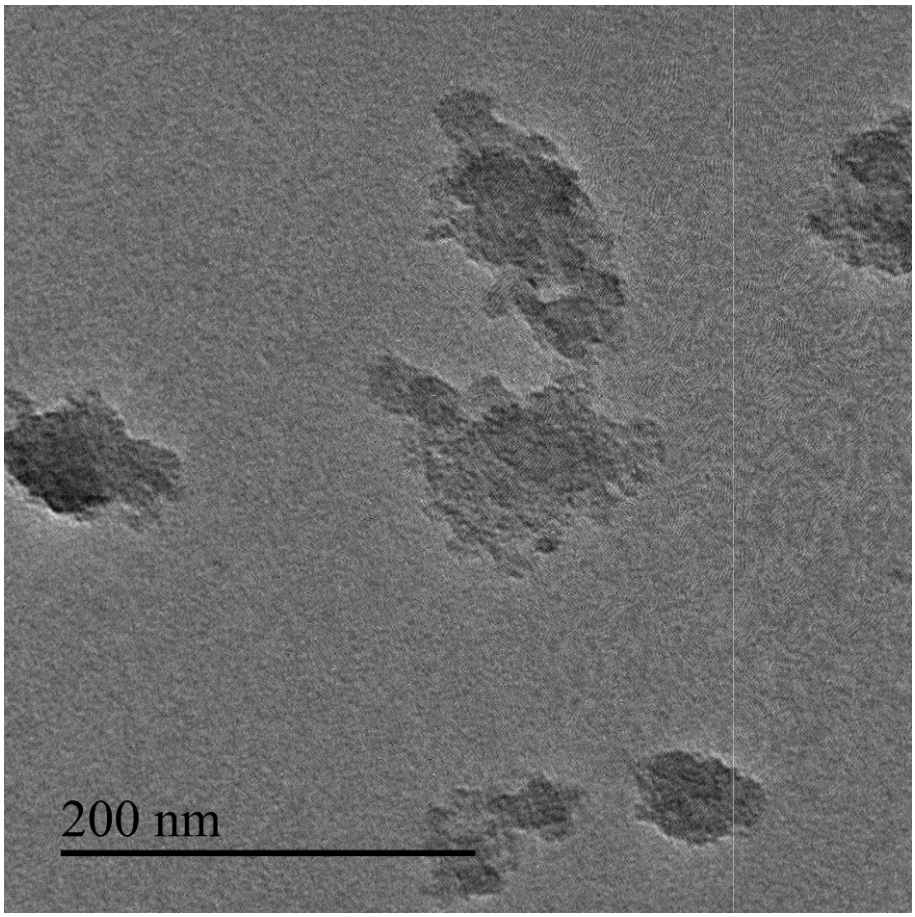

Fig. S4. TEM images of MgO_2.

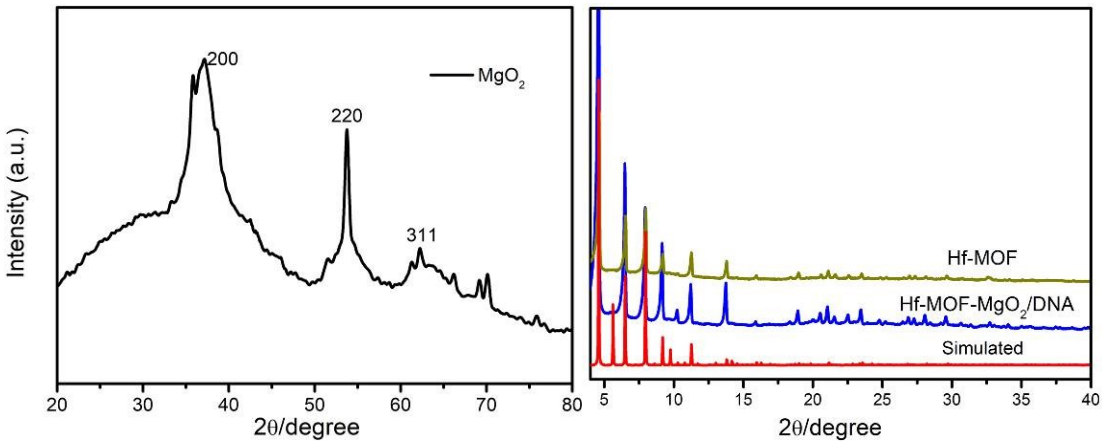

Fig. S5. PXRD patterns of MgO_2, Hf-MOF, Hf-MOF-MgO_2/DNA and the simulated from the crystal data of PCN-224.

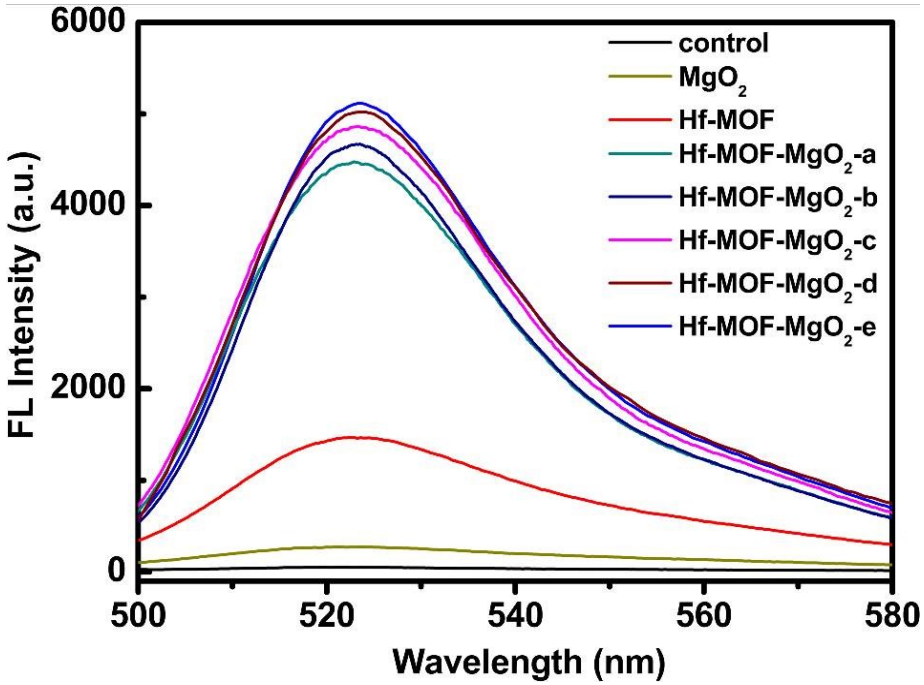

Fig. S6. Fluorescence spectra of DCFH incubated with MgO_2, Hf-MOF and Hf-MOF-MgO_2 in the presence of light irradiation (Hf-MOF-MgO_2-abcde represents the products when Hf-MOF reacted with different amounts of MgO).

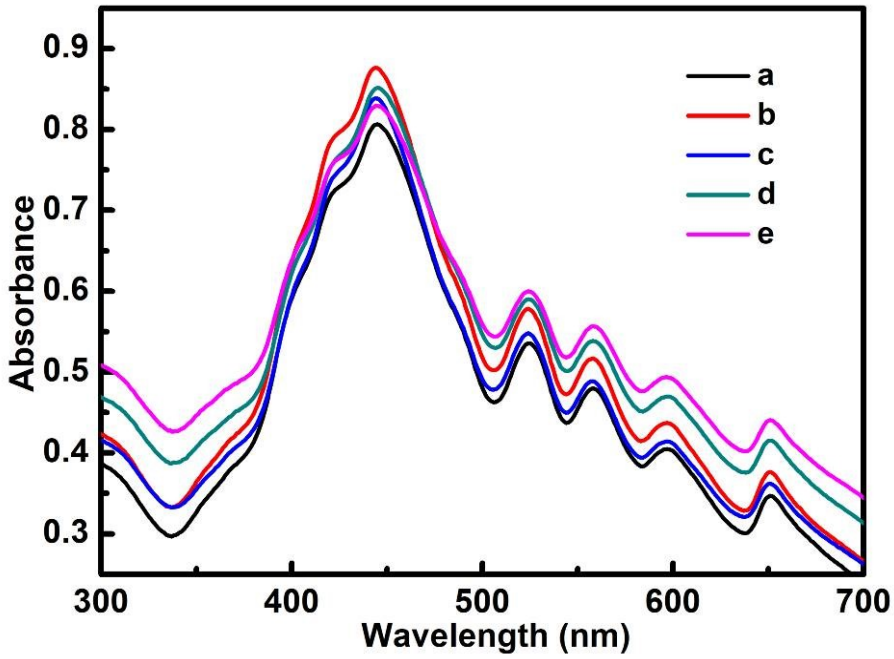

Fig. S7. UV-Vis absorbance of Hf-MOF by combining different amounts of MgO_2.

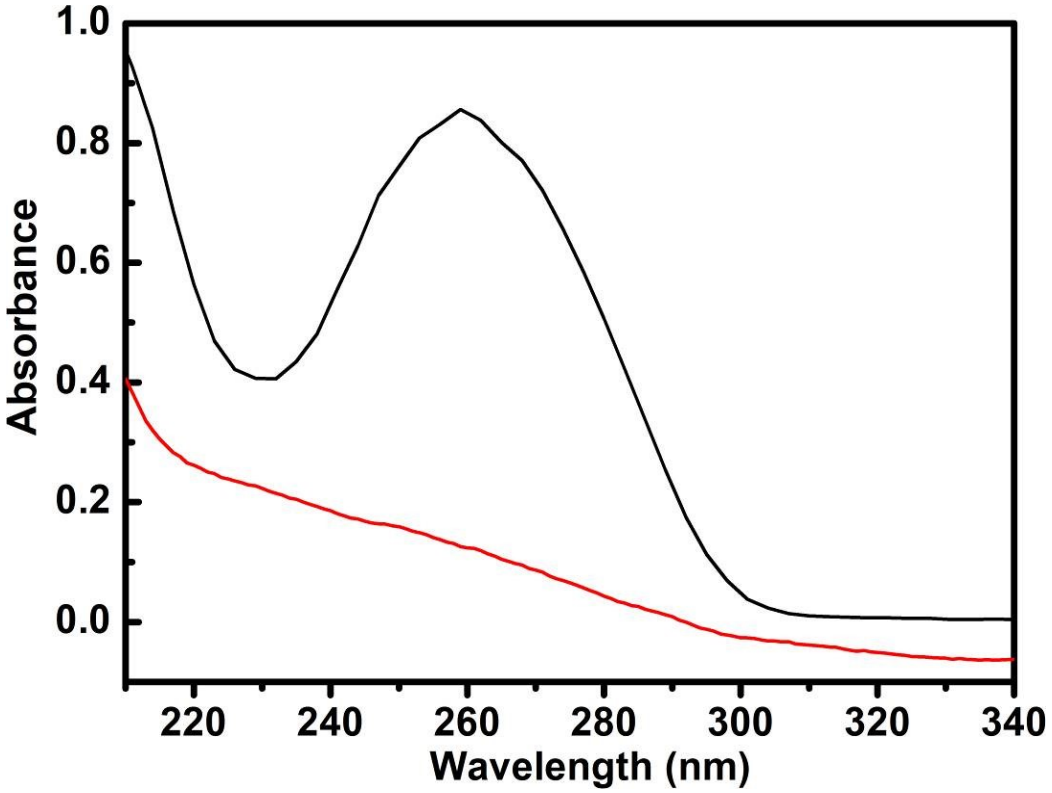

Fig. S8. UV-Vis absorbance of DNA before (black) and after (red) modification with Hf-MOF-MgO_2.

Fig. S9. Images of O_2 bubbles generated by the freshly synthesized (a) MgO_2 and (b) Hf-MOF-MgO_2/DNA in water.

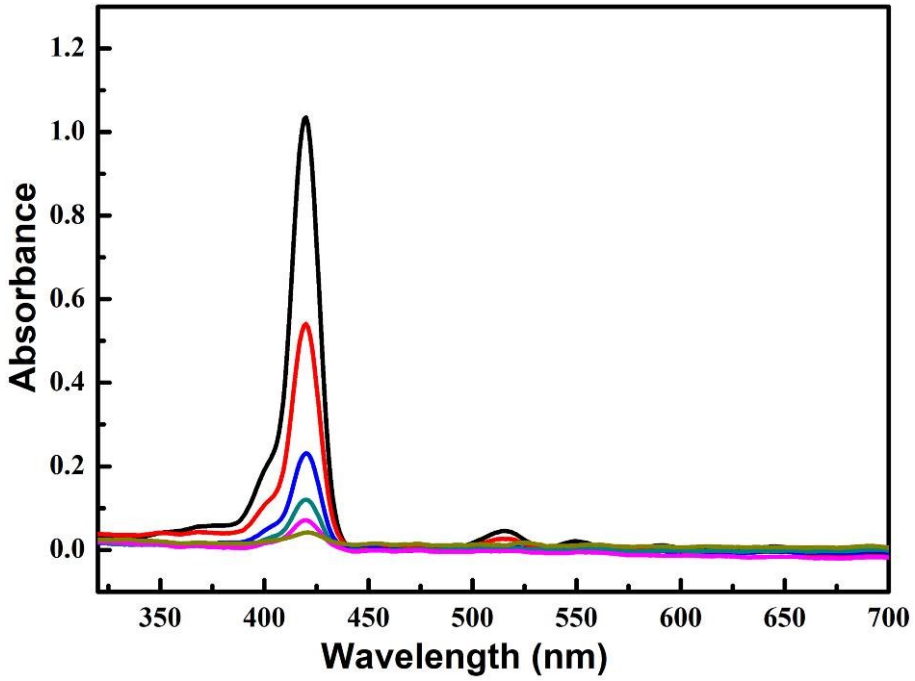

Fig. S10. UV-Vis absorbance spectra of H_2TCPP ligands at different concentration (0.1, 0.5, 1, 2, 5 and 10 μM).

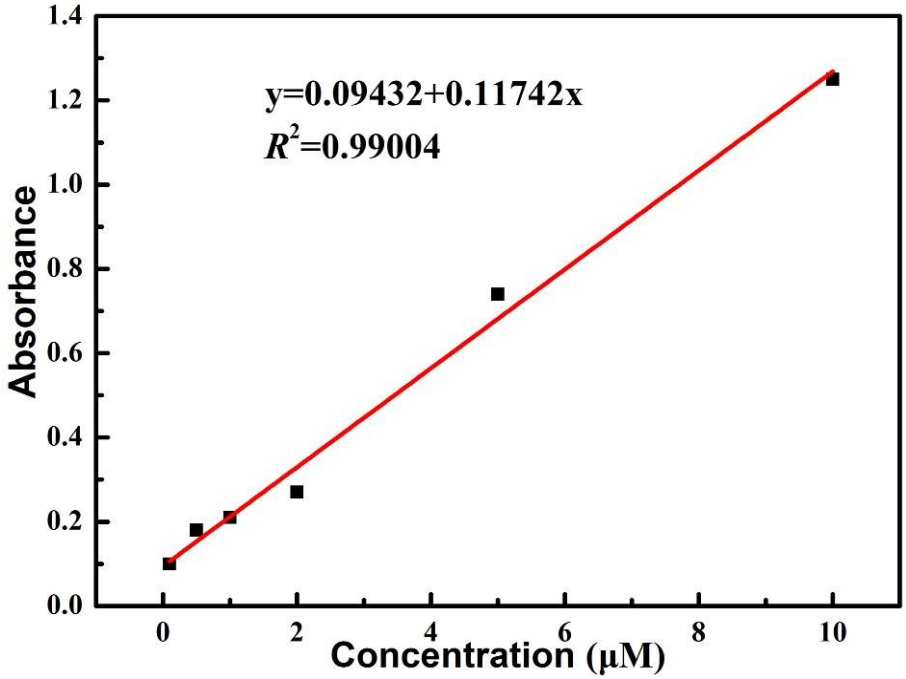

Fig. S11. The calibration curve of absorbance at 418 nm and the concentration of H_2TCPP.

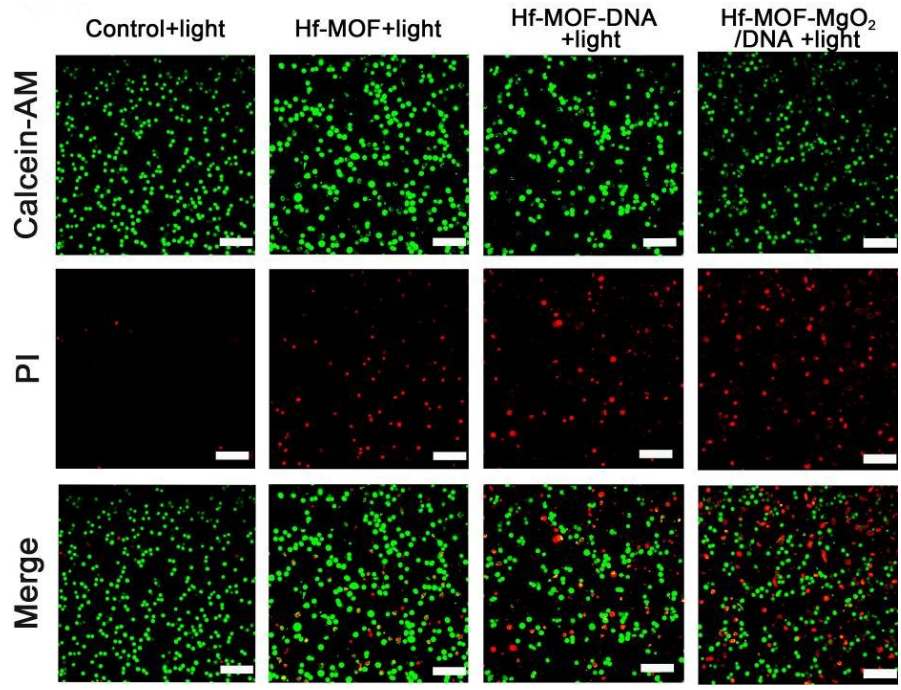

Fig. S12. Confocal images of calcein AM and PI co-stained 4T1 cells treated with different agents under normoxia conditions. Scale bar: 100 μm.

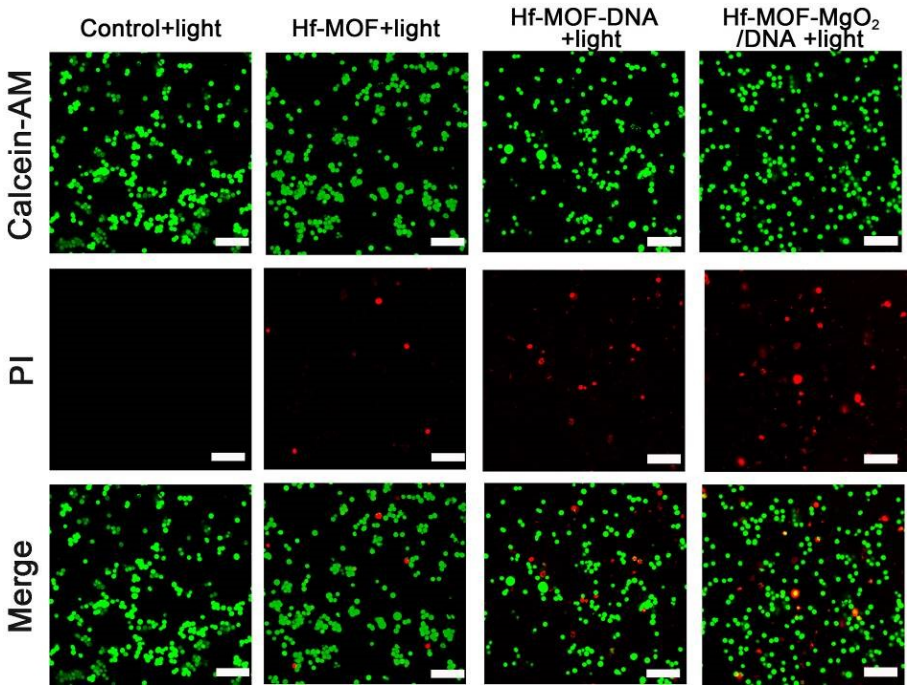

Fig. S13. Confocal images of calcein AM and PI co-stained 4T1 cells treated with different agents under hypoxia conditions. Scale bar: 100 μm.

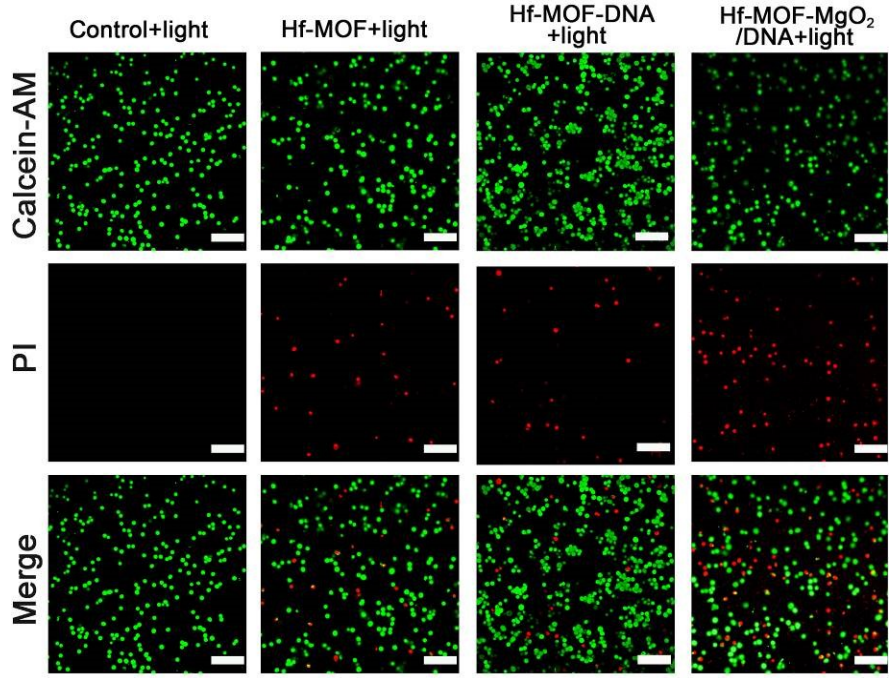

Fig. S14. Confocal images of calcein AM and PI co-stained A549 cells treated with different agents under normoxia conditions. Scale bar: 100 μm.

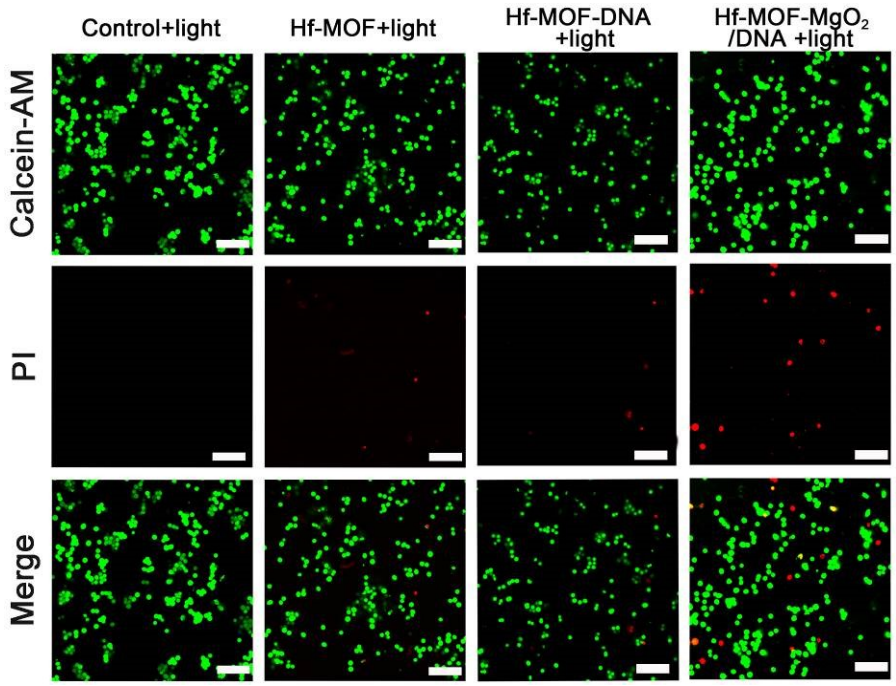

Fig. S15. Confocal images of calcein AM and PI co-stained A549 cells treated with different agents under hypoxia conditions. Scale bar: 100 μm.

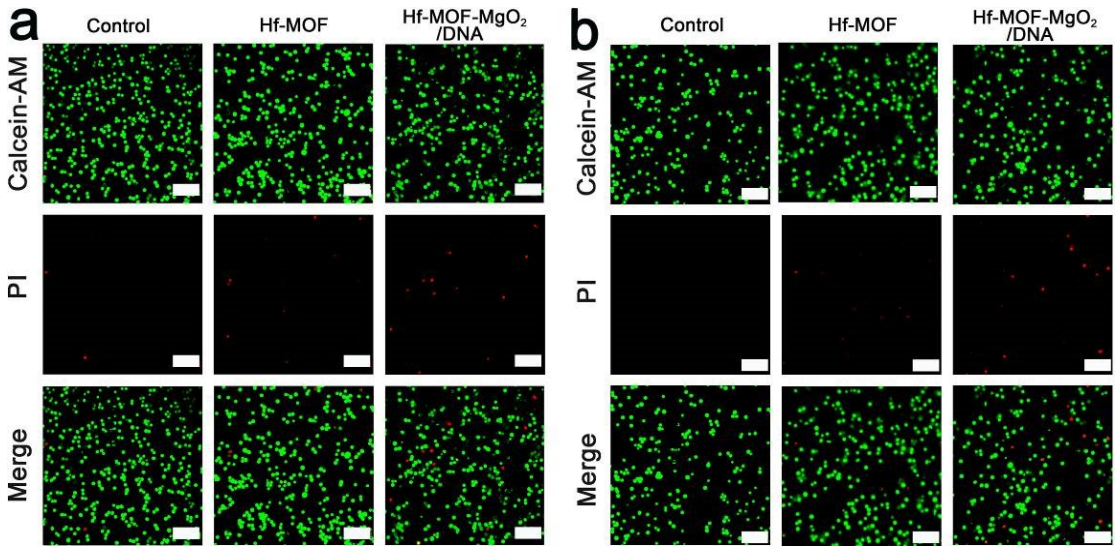

Fig. S16. Confocal images of Calcein-AM/PI stained 4T1 (a) and A549 cells (b) after incubation with Hf-MOF and Hf-MOF-MgO_2/DNA without light irradiation. Scale bar: 100 μm.

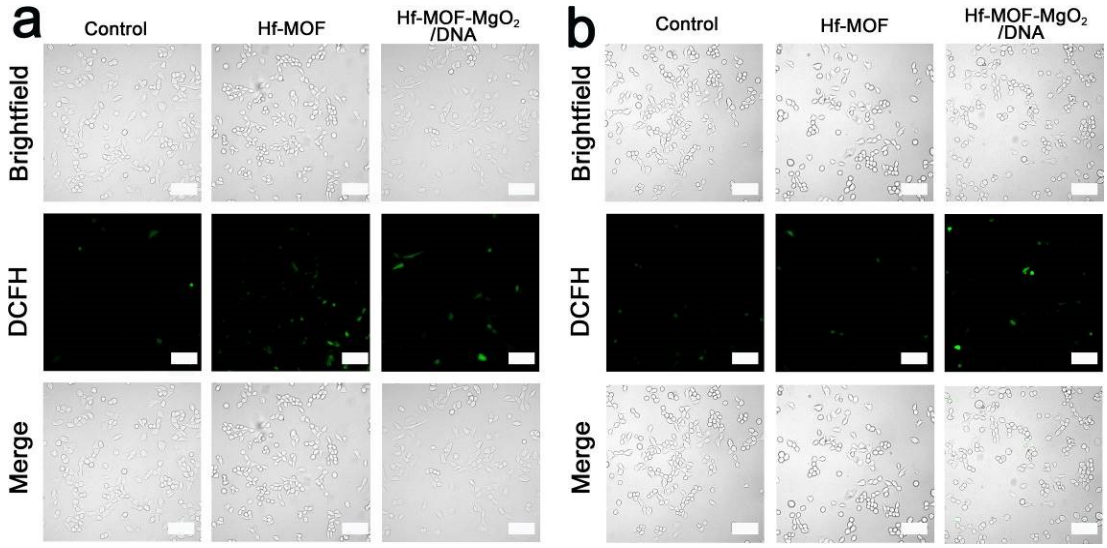

Fig. S17. Confocal images of ROS generation in 4T1 (a) and A549 cells (b) after incubation with Hf-MOF and Hf-MOF-MgO_2/DNA without light irradiation. Scale bar: 100 μm.

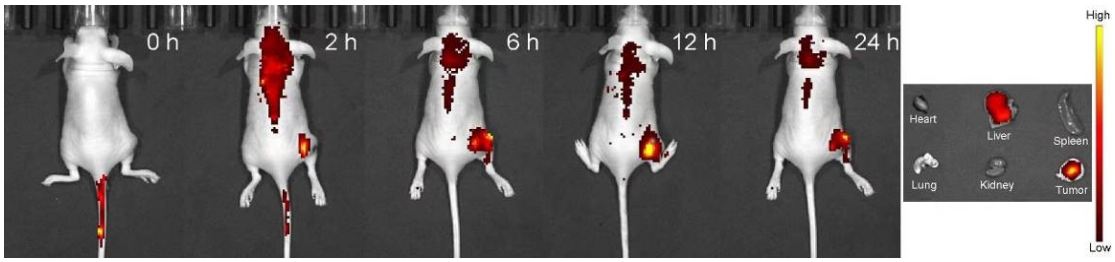

Fig. S18. The fluorescence imaging of 4T1 tumor-bearing mice taken at different time points after intravenous injection with Hf-MOF-MgO_2/DNA and fluorescence imaging of major organs and tumor after intravenous injection at 24 h.

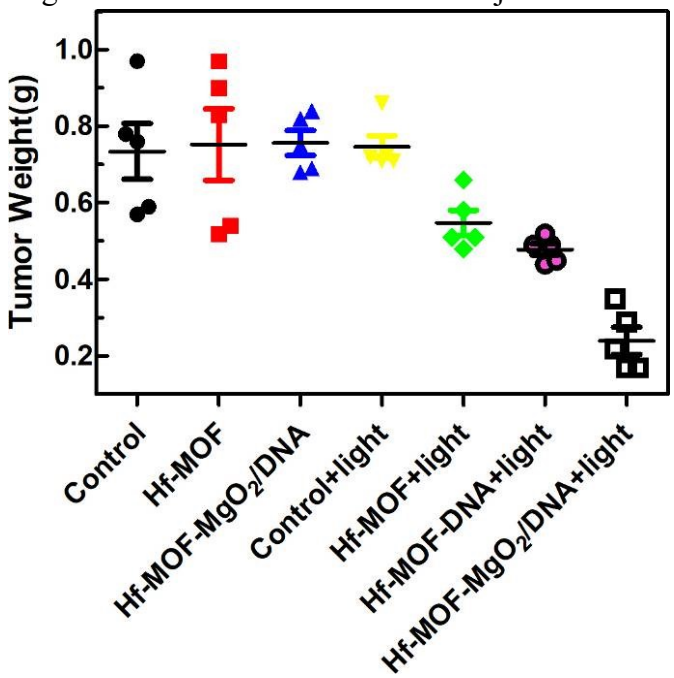

Fig. S19. Tumor weight of different groups after treatment.